Journal of Experimental Botany, Vol. 58, No. 12, pp. 3385–3393, 2007
doi:10.1093/jxb/erm187 Advance Access publication 14 September, 2007

Journal of Experimental Botany
www.jxb.oxfordjournals.org

RESEARCH PAPER

Two members of the *Arabidopsis* CLC (chloride channel) family, AtCLCe and AtCLCf, are associated with thylakoid and Golgi membranes, respectively

Anne Marmagne[1,*,†], Marion Vinauger-Douard[1,*], Dario Monachello[1,‡], Andéol Falcon de Longevialle[1,§], Céline Charon[1,¶], Michèle Allot[1], Fabrice Rappaport[2], Francis-André Wollman[2], Hélène Barbier-Brygoo[1] and Geneviève Ephritikhine[1,3,||]

[1] *Institut des Sciences du Végétal, Centre National de la Recherche Scientifique (CNRS–UPR 2355), Bât 22, avenue de la Terrasse, 91198 Gif sur Yvette Cedex, France*

[2] *Institut de Biologie Physico-Chimique, UMR 7141 CNRS-Université Paris VI, 13 rue Pierre et Marie Curie, 75005 Paris, France*

[3] *Université Paris Diderot Paris7, UFR Biologie Sciences de la Nature, 2 place Jussieu, 75251 Paris cedex 05, France*

Received 13 February 2007; Revised 17 July 2007; Accepted 18 July 2007

Abstract

Though numerous pieces of evidence point to major physiological roles for anion channels in plants, progress in the understanding of their biological functions is limited by the small number of genes identified so far. Seven chloride channel (CLC) members could be identified in the *Arabidopsis* genome, amongst which AtCLCe and AtCLCf are both more closely related to bacterial CLCs than the other plant CLCs. It is shown here that AtCLCe is targeted to the thylakoid membranes in chloroplasts and, in agreement with this subcellular localization, that the *clce* mutants display a phenotype related to photosynthesis activity. The AtCLCf protein is localized in Golgi membranes and functionally complements the yeast *gef1* mutant disrupted in the single *CLC* gene encoding a Golgi-associated protein.

Key words: *Arabidopsis*, CLC chloride channels, Golgi membranes, thylakoids.

Introduction

Anion channels play important roles in plant physiology, but the major limitation to investigating their biological functions originates from our poor knowledge of their molecular identity. Only genes belonging to the CLC (chloride channel) family are known; they were first described in tobacco (Lurin *et al*., 1996). In the *Arabidopsis* genome, seven *CLC* genes could be identified (*AtCLCa–AtCLCg*), and four of them (*AtCLCa*, *-b*, *-c*, and *-d*) have been cloned so far (Hechenberger *et al*., 1996; Geelen *et al*., 2000). The intracellular localization of these four proteins was deduced from expression studies of green fluorescent protein (GFP) fusion proteins in yeast (Hechenberger *et al*., 1996), but direct evidence for their subcellular localization and their transport activity in plant cells was lacking. The physiological characterization of *Arabidopsis* mutants suggested the involvement of AtCLCa (Geelen *et al*., 2000) and AtCLCc (Harada *et al*., 2004) in the regulation of nitrate levels *in planta*. Very recently, the tonoplast localization of AtCLCa and its role as a nitrate/proton antiporter in that membrane was demonstrated, in agreement with its physiological function *in planta* (De Angeli *et al*., 2006).

* These authors contributed equally to this work.
† Present address: UMR de Génétique Végétale, INRA/Université Paris XI/CNRS/INA-PG, Ferme du Moulon, 91190 Gif sur Yvette, France.
‡ Present address: URGV, CNRS-INRA, 2 rue Gaston Crémieux, 91057 Evry cedex, France.
§ Present address: Plant Energy Biology, ARC centre of Excellence, University of Western Australia, 35 Stirling Highway Crawley 6009 WA, Australia.
¶ Present address: Institut de Biotechnologie des Plantes, Université Paris-sud (CNRS-UPS, UMR 8618), Bât. 630, 91405 Orsay cedex, France.
|| To whom correspondence should be addresssed. E-mail: Genevieve.Ephritikhine@isv.cnrs-gif.fr

It is shown here that fusion proteins of AtCLCe and AtCLCf with fluorescent proteins (GFP/DsRed2) are targeted to chloroplasts and Golgi vesicles, respectively, in both onion epidermal cells and *Arabidopsis* protoplasts. Furthermore, western blot analyses revealed the presence of AtCLCe in the thylakoid membranes. Functional data, a photosynthesis-related phenotype for *clce* mutants, and the functional complementation of the yeast *gef1* mutant by AtCLCf are also reported. These results indicate the functionality of the proteins and suggest putative roles in agreement with their subcellular localization.

Materials and methods

Yeast strains, plant material, and culture conditions

All yeast strains were isogenic to the W303 (*ura3-1 can1-100 leu2-3, 112trp1-1 his3-11, 15*) strain. Two strains disrupted by the insertion of the His synthesis gene in the *ScCLC* gene were used in functional complementation tests, the haploid RGY86 and the diploid RGY192 strains (Gaxiola *et al*., 1998). The strains were kindly provided by R Gaxiola (University of Connecticut, Storrs, CT, USA).

Experiments were performed using *Arabidopsis thaliana*, accessions Columbia (Col) or Wassilewskija (WS). Sterilized seeds were grown *in vitro* on standard culture medium ABIS as described by Geelen *et al*. (2000).

Transient expression experiments of GFP fusion proteins were performed on yellow onion bulbs (*Allium cepa*) bought in the local market, or on protoplasts isolated from *Arabidopsis* cell suspensions prepared according the procedure described in Thomine *et al*. (2003).

Yeast transformation and complementation tests

The positive control *AtCLCd* was cloned in the yeast expression vector pRS1024 carrying ampicillin resistance and LEU2 markers (Gaxiola *et al*., 1998). The cDNAs of *AtCLCe* and *AtCLCf* were cloned in pDR195, a yeast expression vector modified according to the Gateway system (Invitrogen), with ampicillin resistance and URA3 as selection marker genes. Yeast transformation was performed using the lithium acetate method (Clontech). Complementation tests were performed in two different discriminating growth conditions as described in Gaxiola *et al*. (1998), basically: (i) a low iron-containing medium (+ 0.6 mM ferrozine, Fluka) at pH 5.8, and (ii) minimal growth media at pH 7 supplemented or not with copper (0.1 mM $CuSO_4$). Each construct was tested in both the haploid RGY86 and the diploid RGY192 yeast strains.

Transient expression of GFP/DsRed2 fusions in onion epidermal cells

The plasmid pSmRSGFP, expressing GFP under the control of the cauliflower mosaic virus 35S promoter, was used for transient expression in onion epidermal cells. It encoded a soluble highly fluorescent variant of jellyfish GFP optimized for use in higher plants (Haseloff *et al*., 1997; Davis and Vierstra, 1998). *AtCLCe* or *AtCLCf* cDNAs were cloned upstream of the GFP and in-frame with GFP in pSmRSGFP using the *Bam*HI site. Different constructs were used to perform co-expression experiments. The SKL22 sequence (Mollier *et al*., 2002), a peroxisomal targeting sequence, and SYTP, a threonyl tRNA synthetase pre-sequence, were fused to DsRed2 in the pOL vector (a gift of I Small, URGV, CNRS-INRA, Evry, France), and used as markers of peroxisomes and plastids/mitochondria, respectively. Biolistic bombardments were performed with a PSD-1000/He instrument (Bio-Rad). Acceleration of gold microcarriers (1.6 μm) coated with 1.25 μg of pure plasmid DNA (purified with Qiagen mini-prep kits) was used to transform onion epidermal cells. Bombardment parameters were as follows: vacuum, 28 inches Hg; distance to target, 6 cm; helium pressure, 650 psi. Onion scales were left for 12–24 h in the dark at 21 °C, and then epidermal tissues were removed and layered in water on glass slides for microscopy.

Transient expression of GFP/DsRed2 fusions in Arabidopsis *protoplasts*

Protoplasts were isolated from *Arabidopsis* cell suspensions, and GFP fusions were transiently expressed in the protoplasts by polyethylene glycol (PEG)-mediated transformation as described in Thomine *et al*. (2003). *AtCLCf* cDNA was introduced in the pOL-DsRed2 vector. Two Golgi markers, α-*1,2 Man99:GFP* (the first 99 amino acids of α-1,2 mannosidase I) (Saint-Jore-Dupas *et al*., 2006) and α-*1,4 FucT:GFP* (α-1,4 fucosyltransferase; unpublished), were kindly provided by V Gomord (UMR 6037, Rouen University); they were used in co-expression experiments with *AtCLCf:DsRed2* fusions.

GFP fluorescence visualization

Confocal microscopy was carried out using a confocal laser-scanning microscope (Leica, confocal system TCS SP2). GFP and YFP (yellow fluorescent protein) fluorochromes were excited by an argon laser at 488 nm and 514 nm, respectively; DsRed2 was excited by a helium–neon laser at 543 nm, and chlorophyll by a helium–neon red laser at 633 nm. Fluorescence was collected between 500 nm and 535 nm for GFP and between 570 nm and 637 nm for DsRed2. In *Arabidopsis* protoplasts, chlorophyll fluorescence was collected between 675 nm and 750 nm.

SDS-PAGE and western blot analyses

Chloroplast subfractions had been prepared from *Arabidopsis* cell suspensions (Ferro *et al*., 2002) and immunologically characterized (Seigneurin-Berny *et al*., 2006); they were kindly provided by N Rolland (CEA/CNRS/UJF/INRA, Grenoble, France). Western blots were performed after SDS-PAGE of chloroplast subfractions (20 μg per fraction), using a purified rabbit antibody raised against AtCLCe synthetic peptides (Eurogentec) at a 1:1000 dilution for 3 h. The rat anti-CLC3 (Sigma) was used at a 1:300 dilution for 3 h.

Screening for T-DNA insertion mutants by PCR

A primary PCR screen was performed on pooled genomic DNA from 45 312 independently isolated T-DNA-transformed Wassilewskija (WS) lines (Bechtold *et al*., 1993; Bouchez *et al*., 1993). Twelve pairs of primers were used, each including an *AtCLCe* gene-specific primer distributed all over the gene and a T-DNA-specific primer for the left and right borders of the T-DNA. A series of PCR screenings on hyperpools (768 lines per pool), superpools (364 lines per pool), pools (48 lines per pool), and finally 48 independent lines subsequently led to the identification of the line of interest, *clce-1*. Searches in several mutant collections led to the identification of another allele, *clce-2*, in the SALK collection (SALK 010237; Columbia accession, Col). Each selected homozygous line was back-crossed using wild-type pollen. New homozygous mutant lines were then produced for their phenotypic characterization. During that work, no *clcf* mutant was identified in the course of the PCR screening of DNA pools.

Fluorescence measurements

The fluorescence induction kinetics were measured with a home-built set-up described in Rappaport *et al*. (2007). Briefly, leaves were cut and illuminated by continuous light (5300 μE m^{-2} s^{-1} light intensity) provided by electroluminescent diodes peaking at

520 nm (35 nm full width at half-maximum). The fluorescence was measured with a photodiode. Band-pass filters were used to cut off the 520 nm light and select the fluorescence light. Prior to the measurement, plants were dark-adapted for 2 h in order to allow the deactivation of the Benson–Calvin cycle.

Results and discussion

AtCLCe and AtCLCf proteins are closely related to prokaryotic CLC channels

AtCLCe (chromosome IV) and *AtCLCf* (chromosome I) genes show different gene structures, with six and eight exons, respectively. Southern blot analyses revealed that these genes are present as single copies in the genome of two different *Arabidopsis* accessions, Col and WS (data not shown). *AtCLCe* encodes a polypeptide of 709 amino acids with a calculated molecular mass of 75.4 kDa (At4g35440); *AtCLCf* potentially encodes two proteins, a short one with a 62.5 kDa calculated molecular mass (586 amino acids; At1g55620.1) and a longer one with a calculated molecular mass of 83.5 kDa (781 amino acids; At1g55620.2).

The AtCLCe and AtCLCf proteins are highly hydrophobic as they showed up to 12 membrane-spanning domains, in agreement with the crystallographic structure of two bacterial CLCs resolved by high resolution X-ray and revealing the existence of 18 α-helices (Mindell *et al*., 2001; Dutzler *et al*., 2002). In the phylogenic tree based on protein sequence comparisons (Fig. 1), most plant CLCs, including those of *Arabidopsis*, belong to a eukaryotic branch, except AtCLCe which defines a distinct subfamily with AtCLCf and some tomato and rice CLCs, all closely related to bacterial CLC proteins. The AtCLCe protein sequence displays 41% amino acid identity with AtCLCf, and 24–34% identity with animal and other plant CLC proteins. The large CLC family includes anion channels such as the torpedo-fish CLC0 (Miller and White, 1980) and the mammalian CLC1 (Steinmeyer *et al*., 1991), but also proton-coupled chloride transporters such as the bacterial CLCec1 (Accardi and Miller, 2004) and the mammalian CLC-4 and CLC-5 (Picollo and Pusch, 2005). A refined analysis of structure/transport mechanism relationships pointed out the key role of two glutamate residues in the Cl^--binding region, E148 and E203, the latter being a hallmark that distinguishes antiporters from channels (Miller, 2006). In plants, demonstration of the antiporter activity of AtCLCa as a nitrate/proton exchanger occurred very recently (De Angeli *et al*., 2006). The AtCLCa sequence displays the two glutamate residues as well as AtCLCb, -c, -d, and -g, while both AtCLCe and AtCLCf possess only E148, suggesting a different transport mechanism.

The AtCLCe protein resides in chloroplasts

The ARAMEMNON database (http://aramemnon.botanik.uni-koeln.de/) did not give strong predictions for the subcellular localization of AtCLCe either in chloroplasts (0.49) or in mitochondria (0.39). Nevertheless, a close analysis of the N-terminal region (MAATLPLCAALRSPVSSRRF) indicated a global positive charge, enrichment in serine and in proline, and the presence of an alanine in the second position; altogether, these features are in favour of a plastid localization. The maximum cleavage site was predicted between the amino acids S17 and R18.

Transient expression in onion epidermal cells of a control construct containing GFP alone resulted in fluorescence throughout the cytosol and within the nucleus (Fig. 2A), as already reported by Haseloff *et al.* (1997). *AtCLCe:GFP* expression resulted in a dotted fluorescence pattern, restricted to mobile organelles located in the cytosol with a diameter of about 3 μm (Fig. 2B), suggesting a plastid localization (leucoplasts in the case of onion epidermal cells; Carde, 1984). Co-expression of *AtCLCe:GFP* with *SYTP:Ds-Red*, which is targeted to both mitochondria and plastids, revealed that green and red fluorescence co-localized to a high degree in plastids (Fig. 2C–E). In addition, upon transient expression of the *AtCLCe:GFP* construct in protoplasts from *Arabidopsis* cell suspensions, a co-localization of the fusion protein (green fluorescence) and chlorophyll (red fluorescence) was observed (Fig. 2F–H), demonstrating the chloroplast targeting of AtCLCe. To localize AtCLCe further, western blot analyses were performed on chloroplast subfractions using both anti-CLC3, an antibody directed against the rat CLC3, and a purified IgG raised against two C-terminal regions of the AtCLCe protein. The patterns obtained with anti-CLC3 could not be interpreted as it cross-reacted with peptides in chloroplasts, envelope, and stroma fractions (data not shown), but blots with anti-CLCe IgGs confirmed the chloroplast localization and showed that AtCLCe resides specifically in thylakoid membranes (Fig. 2I). Interestingly, from transcriptomics data available in Genevestigator tools (http://www.genevestigator.ethz.ch/at/), *AtCLCe* expression is higher in green tissues compared with roots. In seedlings, *AtCLCe* is expressed almost four times more in cotyledons than in roots, and at an intermediate level in hypocotyls (anatomy data sets). In other respects, looking for functional clues, the mutant gene-chip data sets show up-regulation of *AtCLCe* in *lec1* (~2-fold), a leaf developmental mutant, and in a *gun1 gun5* double mutant (~3-fold) altered in plastid signalling pathways during de-etiolation. In contrast, *AtCLCe* expression is down-regulated (~2-fold) in the *pho3* mutant, in which carbon metabolism is affected. Altogether, these data would support a relationship between green tissue thylakoid localization of AtCLCe and a potential function in chloroplasts. This hypothesis was further investigated searching for a photosynthetic phenotype in *clce* mutants.

Mutant clce *plants display altered photosynthetic activity*

clce-1 and *clce-2* homozygous mutant plants exhibit developmental and morphological traits similar to those of

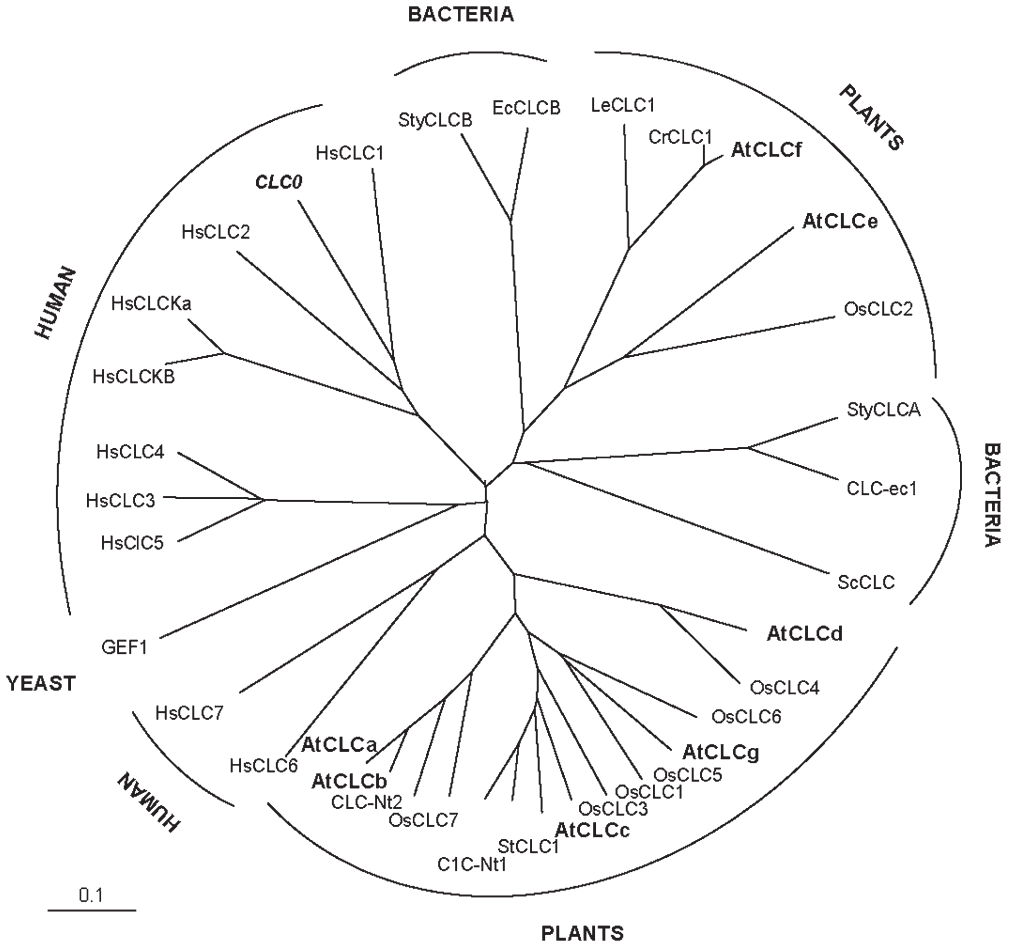

Fig. 1. The plant CLC members are spread over two distinct subfamilies. The dendrogram indicates the degree of similarity between CLC proteins from animals, yeast, bacteria, and plants: CLC0 (P35522) from *Torpedo marmorata*; HsCLC1 (P35523), HsCLC2 (P51788), HsCLC3 (P51790), HsCLC4 (P51793), HsCLC5 (P51795), HsCLC-6 (P51797), HsCLC7 (P51798), HsCLCKa (P51800), and HsCLCKb (P51801), all from *Homo sapiens*; StyCLCA (Q8ZRP8/AAL19167) and StyCLCB (AAL20409) from *Salmonella typhimurium*; GEF1 (P37020) from the yeast *Saccharomyces cerevisiae*; CLC-ec1/EcCLCA (P37019) and EcCLCB (P76175) from *Escherichia coli*; SCLC (P74477) from *Synechocystis* sp.; CLCNt1 (Q881F4) and CLCNt2 (Q9XF71) from *Nicotiana tabacum*; AtCLCa (P92941), AtCLCb (P92942), AtCLCc (Q96282), AtCLCd (P92943), AtCLCe (Q8GX93), AtCLCf (Q8RXR2), and AtCLCg (P60300) all from *Arabidopsis thaliana*; StCLC1 (P93567) from *Solanum tuberosum*; LeCLC (Q9ARC6) from *Lycopersicon esculentum*; and OsCLCa1 (Os01g65500), OsCLC2 (Os01g50860), OsCLC3 (Os02g35190), OsCLC4 (Os03g48940), OsCLC5 (Os04g55210), OsCLC6 (Os08g20570), and OsCLC7 (Os12g25200), all from *Oryza sativa*. *Arabidopsis* CLCs are represented in boldface. All CLC proteins are identified by Swiss-Prot/TrEMBL references (updated version from 2006), except rice CLCs. In that case, CLC-type channel homologous genes were identified in the rice genomic database at NCBI (http://www.tigr.org) and correspond to the classification reported by Diédhiou and Golldack (2006). Programs used were CLUSTAL X (Thompson *et al*., 1997) for whole protein sequence alignments and TreeView (Page, 1996) for graphical output.

wild-type plants grown either *in vitro* or in the greenhouse (data not shown). Looking for a specific phenotypic trait of *clce* mutants which could be related to the chloroplast localization of the protein, chlorophyll fluorescence was measured to assess the photosynthetic activity *in vivo*.

High light intensities induced a strongly polyphasic fluorescence time-course, as previously observed (Delosme, 1967), when the photochemical rate, i.e. the reduction rate of Q_A, is faster than the Q_A^- reoxidation rate (Fig. 3). The first initial rising phase reflects essentially the reduction of Q_A (reviewed in Schreiber, 2002) and, for a given light intensity, its rate is determined by the photosystem II (PSII) antenna size and the photochemical properties of PSII. The half-time of this phase was similar in *clce-1*, *clce-2*, and wild-type plants, indicating that the light trapping efficiency of PSII was unaffected by the mutation. Consistent with this, the PSII quantum yields, as determined by the ratio $(F_m–F_0)/F_m$ (Genty *et al*., 1989), where F_0 and F_m, respectively, stand for the fluorescence yield when all PSIIs are photochemically active and inactive, were similar (0.82 ± 0.3, 0.80 ± 0.4 for the wild type and mutants, respectively). Interestingly, the *clce-1* and *clce-2* mutants displayed a marked phenotype, with the fluorescence increase component, developing in the 10 ms time range, being significantly slowed down, whereas the subsequent phase, occurring in the 100 ms time range, remained unaltered (Fig. 3). As discussed in Schansker *et al*. (2005), these two phases reflect the

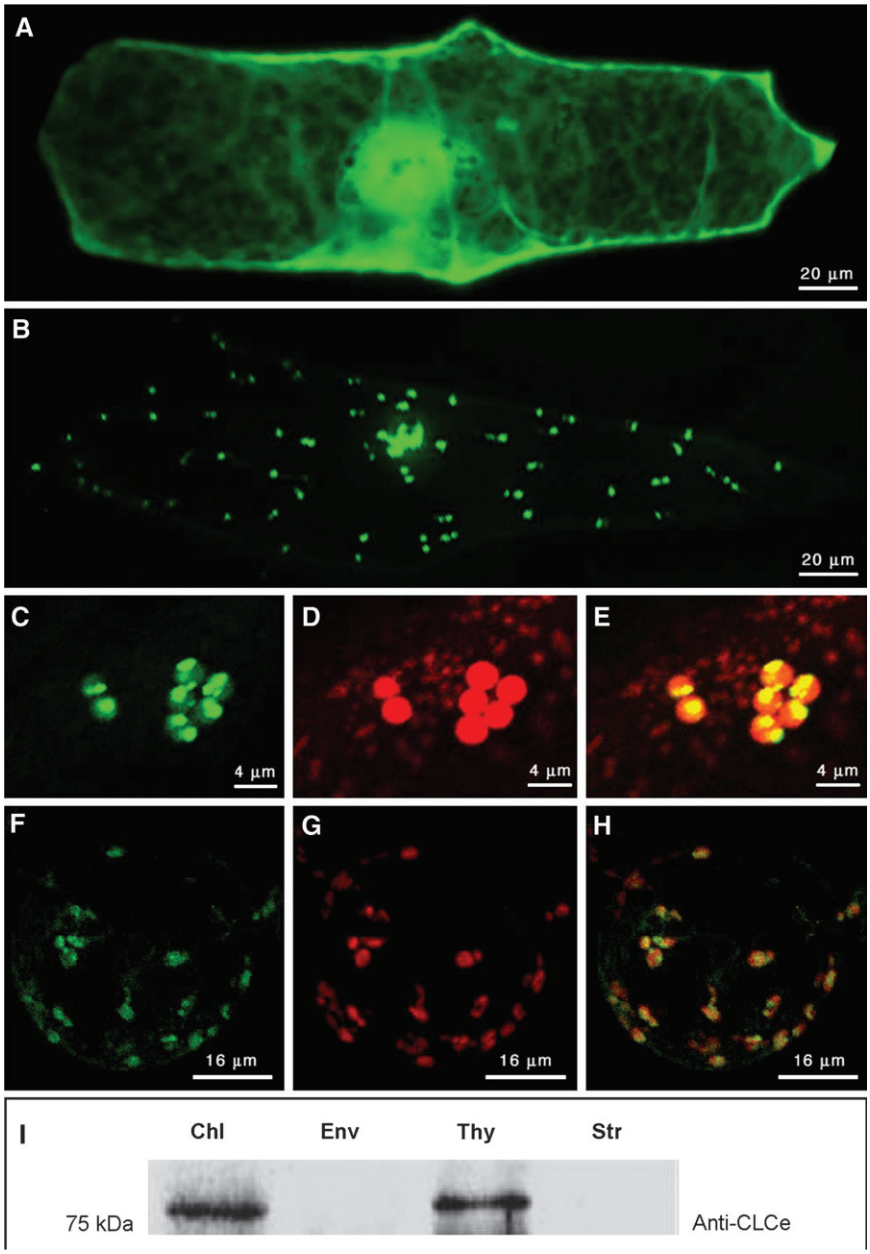

Fig. 2. The AtCLCe protein is targeted to chloroplasts and resides in thylakoid membranes. (A–H) Confocal microscopy analysis of the transient expression of various protein fusions in onion epidermal cells 24 h after bombardement (GFP fusions, A and B, co-expression of GFP and DsRed2 fusions, C–E) and in PEG-transformed *Arabidopsis* protoplasts (GFP fusions, F–H). (A and B) Results from the horizontal projection of different images. (C–H) Unique sections. The white bar indicates the scale in one dimension (µm). (A) Control GFP; (B, C, and F) AtCLCe:GFP fusion; (D) SYTP:DsRed2 fusion, a chloroplast/mitochondria marker; (G) chlorophyll fluorescence; E and H show merges of C (AtCLCe:GFP)/D (SYTP:DsRed2) and F (AtCLCe:GFP)/G (chlorophyll) images, respectively. (I) Western blot analysis of four different fractions, chloroplasts (Chl), envelope (Env), thylakoid (Thy), and stroma (Str). The IgG raised against AtCLCe immunogenic peptides revealed a specific signal in thylakoid membranes, at the expected size.

disappearance of a quencher concomitant with the reduction of the plastoquinone pool, for the first one, and with the reduction of the soluble PSI electron acceptors, for the subsequent one. It is unlikely that AtCLCe activity has direct consequences on the plastoquinone pool *per se*. It is thus proposed that the alterations in the kinetics of fluorescence changes induced by the illumination of dark-adapted *clce* mutant leaves originate from indirect effects, such as changes in the ionic strength or osmotic properties of the lumen resulting from an impaired anionic permeability of the thylakoid membrane. A CLC-type protein might contribute to anion channel activities previously reported on thylakoid membranes by Schönknecht *et al.* (1988) in the higher plant *Peperomia metallica*, and by

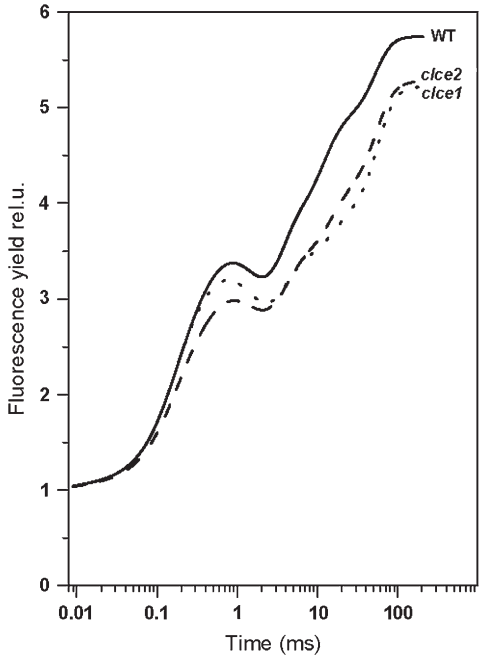

Fig. 3. The *clce* mutants display photosynthesis-related phenotypes. Polyphasic fluorescence increases as a function of the illumination time. The light intensity was 5300 μE m^{-2} s^{-1}. The leaves from plants dark-adapted for 2 h were cut and immediately used for the experiments. Fluorescence changes were measured on leaves harvested from *clce-1* and *clce-2* mutants and wild-type plants, WS and Col, respectively. Wild-type genotypes present the same pattern. The traces are representative of five different experiments performed with leaves from five different plants.

Potossin and Schönknecht in the alga *Nitellopsis obtusa* (1995, 1996), but no direct evidence for such anion currents in *Arabidopsis* photosynthetic thylakoid membranes has been provided so far. Such modifications in the intra-thylakoid ionic status could modify the overall architecture of the thylakoid, and hence the reduction of the plastoquinone pool, since the formation of the grana stacks is known to depend on the ionic strength.

The AtCLCf protein is targeted to Golgi vesicles

AtCLCf:GFP fluorescence in onion epidermal cells was localized in numerous small (1 μm diameter) organelles showing a Brownian movement throughout the cytosol (Fig. 4A). The size of these structures allowed plastids to be excluded, but could correspond to several types of organelles, mitochondria, peroxisomes, or Golgi vesicles. Co-expression of *AtCLCf:GFP* with *SYTP:Ds-Red* (Fig. 4B) led to the exclusion of mitochondrial and chloroplastic locations, as green and red fluorescences did not overlap. Similarly, the green fluorescence of AtCLCf:GFP did not match the distribution of the red fluorescence displayed by a fusion protein targeted to peroxisomes, SKL22:Ds-Red (Fig. 4C). Treatment of onion epidermal cells expressing *AtCLCf:GFP* with brefeldin-A (BFA), a potent inhibitor of endocellular traffic, induced aggregation and redistribution of the green fluorescence (data not shown), suggesting that the AtCLCf:GFP protein was associated with a BFA-sensitive compartment. This observation is in agreement with a Golgi targeting of the AtCLCf protein.

To analyse further the subcellular compartmentation of AtCLCf, transient co-expression of AtCLCf:DsRed2 fusions with fluorescent markers of *cis*- and *trans*-Golgi cisternae was achieved in protoplasts from *Arabidopsis* cell suspensions. In tobacco leaves transformed by agro-infection, the α-1,2 mannosidase I is localized in both endoplasmic reticulum (ER) and *cis*-Golgi subcompartments (Saint-Jore-Dupas *et al*., 2006). In the present biological system, *Man99:GFP* also showed a dual compartmentation (Fig. 4D). Red fluorescence of *AtCLCf:DsRed2* (Fig. 4E) and green fluorescence of *Man99:GFP* (Fig. 4D) completely co-localized in *cis*-Golgi vesicles, but not in the ER (Fig. 4F), suggesting a targeting of AtCLCf to the early Golgi compartment. Co-expression of AtCLCf with a protein targeted to *trans*-Golgi cisternae (Saint-Jore-Dupas *et al*., 2006) was also performed. A partial co-localization was observed between a *trans*-Golgi marker, *FucT:GFP* (V Gomord and M-C Kiefer-Meyer, personal communication) (Fig. 4G), and *AtCLCf:DsRed2* (Fig. 4H, I). Similar fluorescence patterns were obtained when co-expressing *AtCLCf:GFP* and *ST:DsRed2* (the first 52 amino acids of the sialyl transferase) fusions (data not shown). These results obtained in a homologous expression system confirm that AtCLCf would reside in Golgi vesicles. A refined analysis revealed that the fusion protein is mainly targeted to the early *cis*-Golgi subcompartment, and to some extent to *trans*-Golgi cisternae. This result contrasts with a report on the chloroplast localization in spinach of a putative CLC channel sharing sequence similarity with AtCLCf (Teardo *et al*., 2005). In this study, biochemical and mass spectrometry analyses relied on the use of a combination of heterologous tools that may lead to confusing results. The authors themselves do not exclude the hypothesis of the simultaneous presence of CLCf and/or CLCe in other subcellular compartments in spinach.

The present confocal microscopy analyses revealed that in *Arabidopsis*, AtCLCe and AtCLCf reside in different membrane systems, i.e. thylakoid and Golgi membranes, respectively, suggesting that these proteins might play distinct biological roles.

AtCLCf functionally complements the yeast gef1 *mutant*

The yeast CLC protein, ScCLC, has been localized in the Golgi apparatus, most of the protein residing in its medial portion (Gaxiola *et al*., 1998; Schwappach *et al*., 1998) but also in the late- or post-Golgi vesicles (Gaxiola *et al*., 1999). Disruption of the *ScCLC* gene in yeast (*gef1* mutant) led to a growth defect on iron-limited medium

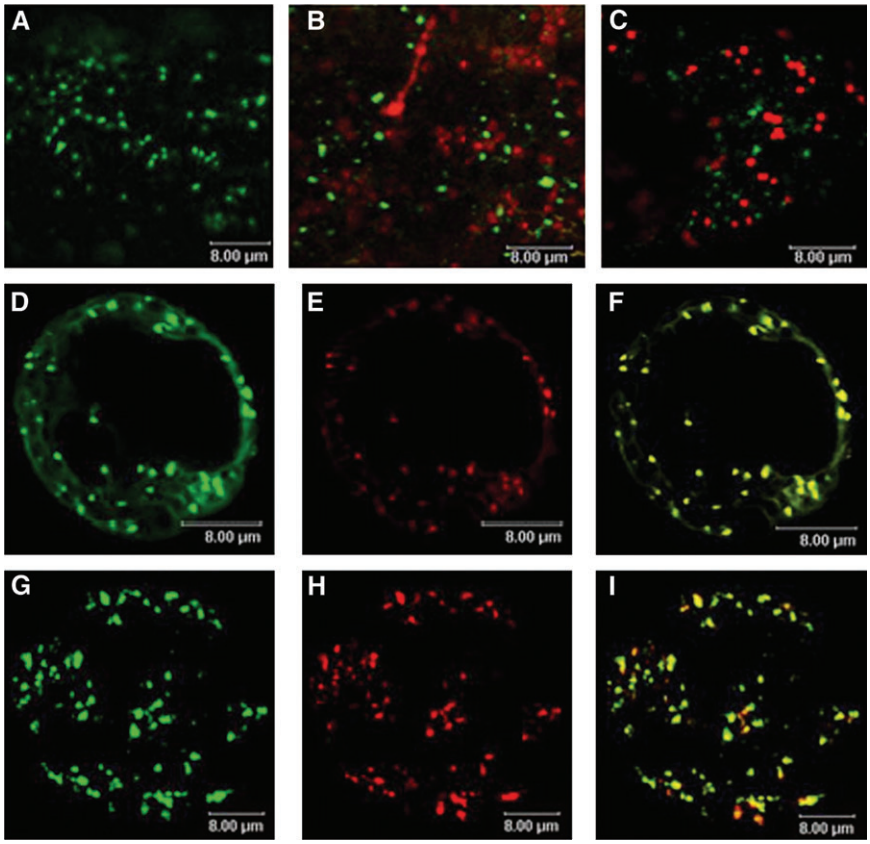

Fig. 4. The AtCLCf protein is targeted to the Golgi membranes. Confocal microscopy analysis of the transient expression of various protein fusions in onion epidermal cells 24 h after bombardement. (A) GFP fusions; (B, C) co-expression of GFP and DsRed2 fusions; (D–I) co-expression of GFP and DsRed2 fusions in PEG-transformed *Arabidopsis* protoplasts. (A) AtCLCf:GFP fusions; (B) merge of AtCLCf:GFP and co-expressed fusions of a chloroplast/mitochondria marker SYTP:DsRed2; (C) co-expression of AtCLCf:GFP and fusions of a peroxisome marker SKL22:DsRed2; (F) merge of (E) AtCLCf:DsRed2/(D) α-1,2 Man99:GFP; (I) merge of (H) (AtCLCf:DsRed2)/(G) α-1,4 FucT:GFP. The white bar indicates the scale in one dimension (µm).

containing non-fermentable carbon sources (Greene *et al*., 1993). AtCLCd was first demonstrated to restore iron-limited growth of the yeast mutant *gef1* (Hechenberger *et al*., 1996). Later on, Gaxiola *et al*. (1998) showed that other phenotypes of the *gef1* mutant, the pH-induced phenotype and salt sensitivity, were also suppressed by complementation with AtCLCd and AtCLCc, but not by AtCLCa. The ability of AtCLCf and AtCLCe functionally to complement growth defects of the mutant strains RGY86 (haploid) and RGY192 (diploid) either on a low-iron medium or on a high pH medium was tested. Figure 5 illustrates the results obtained in the haploid strain RGY86 *gef1*. Similar pictures were obtained for the diploid strain (data not shown). No growth was observed in discriminating growth conditions when yeast strains were transformed with the corresponding empty vectors pDR195 and pRS1024 (data not shown). The *gef1* mutant is unable to grow on non-fermentable carbon sources in the absence of high iron concentrations (Fig. 5A, B). This growth defect is suppressed in *gef1* strains that express the *Arabidopsis CLCf,* but not *AtCLCe* (Fig. 5A, B). The *gef1* mutant also failed to grow on the minimal media SD or SGE, buffered at pH 7 (Fig. 5D, F), though they grew well on a minimal medium YPD (Fig. 5C); this phenotype was also rescued by the expression of *AtCLCf* (Fig. 5D, F). The addition of copper allows growth of all genotypes (Fig. 5E–G), probably because it restores in *gef1* background the high affinity iron uptake through the Fet3–Ccc2 complex (Gaxiola *et al*., 1998). In all discriminating growth conditions, expression of *AtCLCe* did not complement the two yeast mutant strains, probably as a consequence of its chloroplast localization (Fig. 5). In all cases, *AtCLCf* expression in the *gef1* background was able to restore growth of the mutant strains although at a lower rate compared with the wild-type strain or with the positive control represented by the *gef1* strain expressing *AtCLCd* (Fig. 5).

Recently, AtCLCd has been shown to co-localize in the *trans*-Golgi network with VHA-a1, a subunit of the proton-transporting V-type ATPase (Von der Fecht-Bartenbach *et al*., 2007). These data suggest that AtCLCd would be involved in the transport of a counter-anion for compensating acidification of the luminal pH in the trans-Golgi network required during endocytic and secretory

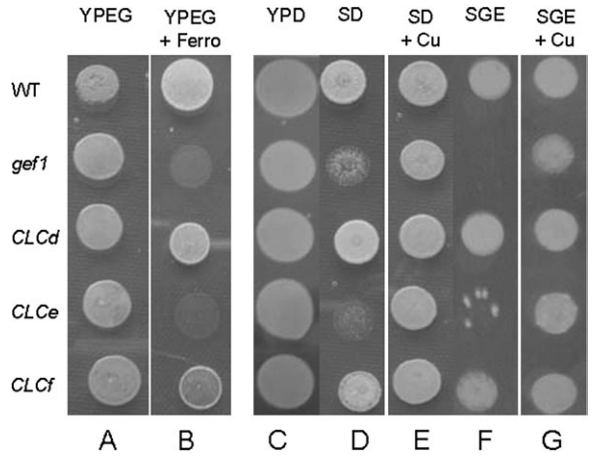

Fig. 5. AtCLCf functionally complements the *gef-1* yeast mutant. Suspensions of the indicated strains W303 (WT), RGY86 (*gef-1* mutant,) and each transformant (*gef-1*:CLCd, *gef-1*:CLCe, and *gef-1*:CLCf) were set up at DO1 (5×10^8 cells). Serial dilutions (d1–d16) were spotted onto the appropriate media. For clarity, the figure illustrates the results obtained with one of the dilutions. For the low-iron phenotype, a 4-fold dilution of each suspension was spotted onto YPEG media supplemented with 0.6 mM ferrozine, pH 5.8 (A, B) and grown for 3 d at 30 °C. The results are representative of four independent experiments. For the pH-dependent phenotype, an 8-fold dilution was spotted onto YPD (C), SD ± 0.1 mM CuSO4, pH 7 (D, E) and SGE ± $CuSO_4$ 0.1 mM, pH 7 (F, G) media and grown for 3 d at 30 °C. The results are representative of two independent experiments.

processes (Dettmer *et al.*, 2006). The present data illustrate that AtCLCf is functional in yeast cells and provide evidence for its ability to complement the pH-dependent growth phenotype of the *gef1* mutant. AtCLCf might thus play a role in delivering anions to facilitate the luminal acidification of the *cis*-Golgi subcompartment.

Concluding remarks

Here the molecular cloning and preliminary biological characterization of *AtCLCe* and *AtCLCf*, two new *Arabidopsis* genes encoding putative plant CLC anion channels, are reported. In contrast to AtCLCa, these two proteins are located in membrane systems which are not easily amenable to electrophysiology techniques, and this hampers progress to demonstrate their genuine channel or transporter activity. However, the identification of the subcellular localization of the proteins in thylakoid or Golgi membranes, together with mutant analysis and yeast complementation assays, provides the first clues as to their cellular functions. Such functions appear specific to plant cells (AtCLCe and photosynthesis) or similar to those described for yeast and some of the mammalian CLCs (AtCLCf and acidification of Golgi or endosomal vesicles) (reviewed in Jentsch, 2007).

Acknowledgements

We thank C Lurin (URGV, CNRS-INRA, Evry, France) and C Maurel (BPMP, Agro-M/INRA/CNRS/UM2 UMR 5004, Montpellier, France) for their help at the beginning of this work, M Thomas (IBP, CNRS-Université Paris Sud 11, Orsay, France) for providing the cDNA library, C Giglione (ISV, CNRS, Gif sur Yvette) for the plasmid pSmRSGFP, R Gaxiola (University of Connecticut, Storrs, CT, USA) for kindly providing yeast strains, N Rolland (PCV, CEA/CNRS/UJF/INRA, Grenoble, France) for chloroplast fractions and the anti-E37 antibody, I Small (URGV, CNRS-INRA, Evry, France) for SYTP:SKL22 and CoxIV:DsRed2 constructs, C Saint-Jore (Rouen University, France), I Moore (Oxford University, UK), and C Hawes (Oxford Brookes University, UK) for the kind gift of ST:YFP, V Gomord, C Saint-Jore-Dupas, and A Boulaflous (UMR 6037, University of Rouen, France) for kindly providing a new set of Golgi markers, α-1,2 Man99:GFP and α-1,4 Fuct:GFP, and for helpful discussions on subcellular localization experiments, and S Brown and C Talbot for offering confocal microscopy facilities of the Cell Biology Platform of IFR 87 'La Plante et son Environnement' (ISV, CNRS, Gif sur Yvette, France). This project was supported by the Centre National de la Recherche Scientifique and the Génoplante programme AF1999035. DM was funded by European Research Training Network NICIP CT-2002-000245.

References

Accardi A, Miller C. 2004. Secondary active transport mediated by a prokariotic homologue of ClC Cl^- channels. *Nature* **427,** 803–807.

Bechtold N, Ellis J, Pelletier G. 1993. *In planta Agrobacterium* mediated gene transfer by infiltration of adult *Arabidopsis thaliana* plants. *Comptes Rendu de l'Académie des Sciences Séries III, Sciences de la Vie. Paris* **316,** 1194–1199.

Bouchez D, Camilleri C, Caboche M. 1993. A binary vector based on Basta resistance for *in planta* transformation of *Arabidopsis thaliana*. *Comptes Rendu de l'Académie des Sciences, Séries III, Sciences de la Vie, Paris* **316,** 1188–1193.

Carde J. 1984. Leucoplasts: a distinct kind of organelles lacking typical 70S ribosomes and free thylakoids. *European Journal of Cell Biology* **34,** 18–26.

Davis S, Vierstra R. 1998. Soluble, highly fluorescent variants of green fluorescent protein (GFP) for use in higher plants. *Plant Molecular Biology* **36,** 521–528.

De Angeli A, Monachello D, Ephritikhine G, Frachisse JM, Thomine S, Gambale F, Barbier-Brygoo H. 2006. The nitrate/proton antiporter AtCLCa mediates nitrate accumulation in plant vacuoles. *Nature* **442,** 939–943.

Delosme R. 1967. Étude de l'induction de fluorescence des algues et des chloroplastes au début d'une illumination intense. *Biochimica et Biophysica Acta* **143,** 108–128.

Dettmer J, Hong-Hermesdorf A, Stierhof Y-D, Schumacher K. 2006. Vacuolar H^+-ATPase activity is required for endocytic and secretory trafficking in *Arabidopsis*. *The Plant Cell* **18,** 715–730.

Dhédhiou CJ, Golldack D. 2006. Salt-dependent regulation of chloride channel transcripts in rice. *Plant Science* **170,** 793–800.

Dutzler R, Campbell EB, Cadene M, Chait BT, Mackinnon R. 2002. X-ray structure of CLC chloride channel at 3.0 Å reveals the molecular basis of anion selectivity. *Nature* **415,** 287–294.

Ferro M, Salvi D, Rivière-Rolland H, Vermat T, Seigneurin-Berny D, Grunwald D, Garin J, Joyard J, Rolland N. 2002. Integral membrane proteins of the chloroplast envelope: identification and subcellular localization of new transporters. *Proceedings of the National Academy of Sciences, USA* **99,** 11487–11492.

Gaxiola RA, Rao R, Sherman A, Grisafi P, Alper SL, Fink GR. 1999. The *Arabidopsis thaliana* proton transporters, AtNhx1 and Avp1, can function in cation detoxification in yeast. *Proceedings of the National Academy of Sciences, USA* **96,** 1480–1485.

Gaxiola RA, Yuan DS, Klausner RD, Fink GR. 1998. The yeast CLC chloride channel functions in cation homeostasis. *Proceedings of the National Academy of Sciences, USA* **95,** 4046–4050.

Geelen D, Lurin C, Bouchez D, Frachisse JM, Lelievre F, Courtial B, Barbier-Brygoo H, Maurel C. 2000. Disruption of putative anion channel gene *AtCLC-a* in *Arabidopsis* suggests a role in the regulation of nitrate content. *The Plant Journal* **21,** 259–269.

Genty B, Briantais J-M, Baker NR. 1989. The relationship between the quantum yield of photosynthetic electron transport and quenching of chlorophyll fluorescence. *Biochimica et Biophysica Acta* **990,** 87–92.

Greene JR, Brown NH, DiDomenico BJ, Kaplan J, Eide DJ. 1993. The *GEF1* gene of *Saccharomyces cerevisiae* encodes an integral membrane protein; mutations in which have effects on respiration and iron-limited growth. *Molecular and General Genetics* **241,** 542–553.

Harada H, Kuromori T, Hirayama T, Shinozaki K, Leigh RA. 2004. Quantitative trait loci analysis of nitrate storage in *Arabidopsis* leading to an investigation of the contribution of the anion channel gene, *AtCLC-c*, to variation in nitrate levels. *Journal of Experimental Botany* **55,** 2005–2014.

Haseloff J, Siemering K, Prasher D, Hodge S. 1997. Removal of a cryptic intron and subcellular localization of green fluorescent protein are required to mark transgenic *Arabidopsis* plants brightly. *Proceedings of the National Academy of Sciences, USA* **94,** 2122–2127.

Hechenberger M, Schwappach B, Fischer WN, Frommer WB, Jentsch TJ, Steinmeyer K. 1996. A family of putative chloride channels from *Arabidopsis* and functional complementation of a yeast strain with a CLC gene disruption. *Journal of Biological Chemistry* **271,** 33632–33638.

Jentsch TJ. 2007. Chloride and the endosomal–lysosomal pathway: emerging roles of CLC chloride transporters. *Journal of Physiology* **578,** 633–640.

Lurin C, Geelen D, Barbier-Brygoo H, Guern J, Maurel C. 1996. Cloning and functional expression of a plant voltage-dependent chloride channel. *The Plant Cell* **8,** 701–711.

Miller C. 2006. ClC chloride channels viewed through a transporter lens. *Nature* **440,** 484–489.

Miller C, White MMA. 1980. A voltage-dependent chloride conductance channel from *Torpedo electroplax* membrane. *Annals of the New York Academy of Sciences* **341,** 534–551.

Mindell J, Maduke M, Miller C, Grigorieff N. 2001. Projection structure of a ClC-type chloride channel at 6.5 Å resolution. *Nature* **409,** 219–223.

Mollier P, Hoffman B, Debast C, Small I. 2002. The gene encoding *Arabidopsis thaliana* mitochondrial ribosomal protein S13 is a recent duplication of the gene encoding plastid S13. *Current Genetics* **40,** 405–409.

Page RD. 1996. TreeView: an application to display phylogenetic trees on personal computers. *Computer Applications in the Biosciences* **12,** 357–358.

Piccolo A, Pusch M. 2005. Chloride/proton antiporter activity of mammalian proteins CLC-4 and CLC-5. *Nature* **436,** 420–423.

Pottosin II, Shönknecht G. 1995. Patch clamp study of the voltage-dependent anion channel in the thylakoid membrane. *Journal of Membrane Biology* **148,** 143–156.

Pottosin II, Shönknecht G. 1996. Ion channel permeable for divalent and monovalent cations in native spinach thylakoid membrane. *Journal of Membrane Biology* **152,** 223–233.

Rappaport F, Béal D, Joliot A, Joliot P. 2007. On the advantages of using green light to study fluorescence yield changes in leaves. *Biochimica et Biophysica Acta* **1767,** 56–65.

Saint-Jore-Dupas C, Nebenführ A, Boulaflous A, Follet-Gueye M-L, Plasson C, Hawes C, Driouich A, Faye L, Gomord V. 2006. Plant N-glycan processing enzymes employ different targeting mechanisms for their spatial arrangement along the secretory pathway. *The Plant Cell* **18,** 3182–3200.

Schansker G, Toth SZ, Strasser RJ. 2005. Methylviologen and dibromothymoquinone treatments of pea leaves reveal the role of photosystem I in the Chla fluorescence rise OJIP. *Biochimica et Biophysica Acta* **1706,** 250–261.

Schönknecht G, Hedrich R, Junge W, Raschke K. 1988. A voltage-dependent chloride channel in the photosynthetic membrane of a higher plant. *Nature* **336,** 589–592.

Schreiber U. 2002. Assessment of maximal fluoresence: donor-site dependent quenching and QB quenching. In: Van Kooten O, Snel JFH, eds. *Plant spectrofluorometry: applications and basic research*. Amstredam: Rozenberg Publisher, 23–48.

Schwappach B, Stobrawa S, Hechenberger M, Steinmeyer K, Jentsch TJ. 1998. Golgi localization and functionally important domains in the NH_2 and COOH terminus of the yeast CLC putative chloride channel Gef1p. *Journal of Biological Chemistry* **273,** 15110–15118.

Seigneurin-Berny D, Gravot A, Auroy P, *et al*. 2006. HMA1, a new Cu-ATPase of the chloroplast envelope, is essential for growth under adverse light conditions. *Journal of Biological Chemistry* **281,** 2882–2892.

Steinmeyer K, Ortland C, Jentsch TJ. 1991. Primary structure and functional expression of a developmentally regulated skeletal muscle chloride channel. *Nature* **354,** 301–304.

Teardo E, Frare E, Segalla A, De Marco V, Giacometti GM, Szabo I. 2005. Localization of a putative ClC chloride channel in spinach chloroplasts. *FEBS Letters* **579,** 4991–4996.

Thomine S, Lelièvre F, Debarbieux E, Schroeder JI, Barbier-Brygoo H. 2003. AtNRAMP3, a multispecific vacuolar metal transporter involved in plant responses to iron deficiency. *The Plant Journal* **34,** 685–695.

Thompson JD, Gibson TJ, Plewniak F, Jeanmougin F, Higgins DG. 1997. The CLUSTAL X windows interface: flexible strategies for multiple sequence alignment aided by quality analysis tools. *Nucleic Acids Research* **25,** 4876–4882.

Von der Fecht-Bartenbach J, Bogner M, Krebs M, Stierhof Y-D, Schumacher K, Ludewig U. 2007. Function of the anion transporter AtCLC-d in the trans-Golgi network. *The Plant Journal* **50,** 466–474.